Temperature-Induced Reversible First-Order Single Crystal to Single Crystal Phase Transition in Boc-γ 4 (R)Val-Val-OH: Interplay of Enthalpy and Entropy

ARTICLE *in* THE JOURNAL OF PHYSICAL CHEMISTRY A · SEPTEMBER 2014

Impact Factor: 2.69 · DOI: 10.1021/jp506874q · Source: PubMed

5 AUTHORS, INCLUDING:

madhusudana Reddy M B

Indian Institute of Science

22 PUBLICATIONS **171** CITATIONS

SEE PROFILE

Dinesh Bhimareddy

French National Centre for Scientific Research

16 PUBLICATIONS **55** CITATIONS

SEE PROFILE

Padmanabhan Balaram

Indian Institute of Science

507 PUBLICATIONS **14,103** CITATIONS

SEE PROFILE

THE JOURNAL OF PHYSICAL CHEMISTRY A

Article

pubs.acs.org/JPCA

Temperature-Induced Reversible First-Order Single Crystal to Single Crystal Phase Transition in Boc-γ^4(*R*)Val-Val-OH: Interplay of Enthalpy and Entropy

Rumpa Pal,[†] M. B. Madhusudana Reddy,[‡] Bhimareddy Dinesh,[‡] Padmanabhan Balaram,[‡] and Tayur N. Guru Row*[,†]

[†]Solid State and Structural Chemistry Unit, Indian Institute of Science, Bangalore-560012, India

[‡]Molecular Biophysics Unit, Indian Institute of Science, Bangalore-560012, India

Supporting Information

ABSTRACT: Crystals of Boc-γ^4(*R*)Val-Val-OH undergo a reversible first-order single crystal to single crystal phase transition at $T_c \approx 205$ K from the orthorhombic space group $P22_12_1$ ($Z' = 1$) to the monoclinic space group $P2_1$ ($Z' = 2$) with a hysteresis of ~2.1 K. The low-temperature monoclinic form is best described as a nonmerohedral twin with ~50% contributions from its two components. The thermal behavior of the dipeptide crystals was characterized by differential scanning calorimetry experiments. Visual changes in birefringence of the sample during heating and cooling cycles on a hot-stage microscope with polarized light supported the phase transition. Variable-temperature unit cell check measurements from 300 to 100 K showed discontinuity in the volume and cell parameters near the transition temperature, supporting the first-order behavior. A detailed comparison of the room-temperature orthorhombic form with the low-temperature (100 K) monoclinic form revealed that the strong hydrogen-bonding motif is retained in both crystal systems, whereas the non-covalent interactions involving side chains of the dipeptide differ significantly, leading to a small change in molecular conformation in the monoclinic form as well as a small reorientation of the molecules along the *ac* plane. A rigid-body thermal motion analysis (translation, libration, screw; correlation of translation and libration) was performed to study the crystal entropy. The reversible nature of the phase transition is probably the result of an interplay between enthalpy and entropy: the low-temperature monoclinic form is enthalpically favored, whereas the room-temperature orthorhombic form is entropically favored.

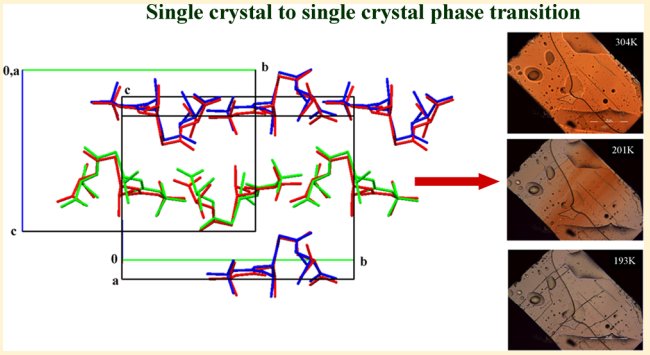

INTRODUCTION

Interest in single crystal to single crystal transformations is growing and the evaluation of their consequences on structure−property relationships has been extensively studied in the literature.[1] While several examples have been reported in cases of inorganic and macroporous materials, such transformations appear to be much less common in organic crystals. A simple search of the Cambridge Structural Database for "phase transition" resulted in 1337 hits. Among them, only ~300 cases are temperature-induced. In the case of amino acids, peptides and complexes, though a few reports on pressure-induced phase transitions have been reported in the literature,[2,3] temperature-induced phase transitions in peptides have not been studied in detail to the best of our knowledge.

While investigating syn/anti conformations of carboxylic acids in oligopeptides, we accidentally observed a temperature-induced single crystal to single crystal reversible first-order phase transition in the hybrid $\gamma\alpha$ peptide Boc-γ^4(*R*)Val-Val-OH (Scheme 1).[4] The reversible nature of the phase transition is best understood in terms of the thermodynamic properties of the system, that is, as an interplay between enthalpy and entropy.

X-ray diffraction studies provide an experimental measure of the thermally averaged ground-state crystal electron density.

Scheme 1. Structure of Boc-γ^4(R)Val-Val-OH with Atom-Labeling Scheme

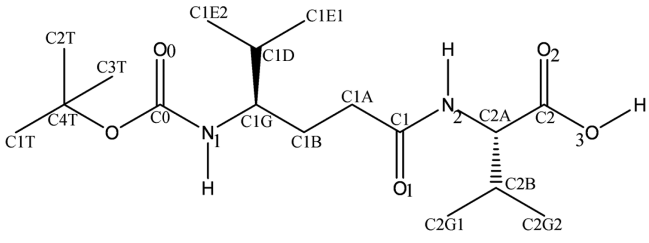

Received: July 10, 2014
Revised: September 5, 2014
Published: September 8, 2014

dx.doi.org/10.1021/jp506874q | *J. Phys. Chem. A* 2014, 118, 9568−9574

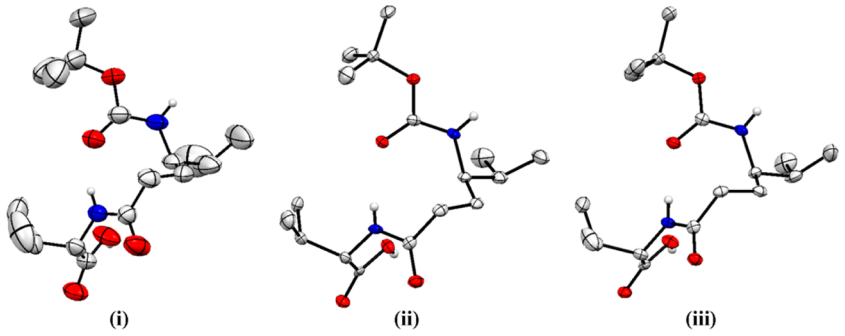

Figure 1. ORTEP diagrams (50% probability ellipsoids) for Boc-γ^4(*R*)Val-Val-OH: (i) MOLRT at 298 K; (ii) MOL1 at 100 K; (iii) MOL2 at 100 K.

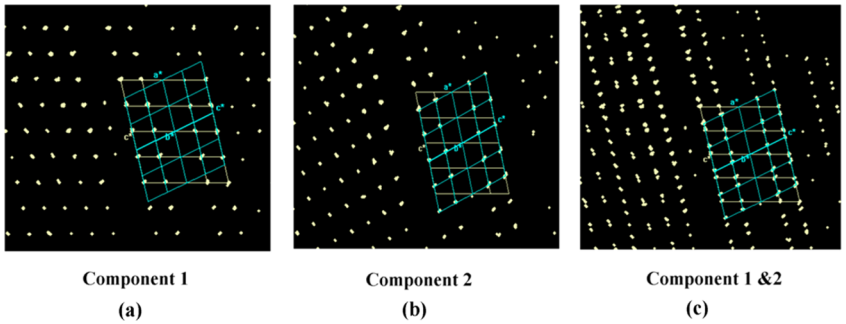

Figure 2. (a, b) Reciprocal-space images showing unit cells corresponding to the two components of the nonmerohedral twin $P2_1$ as viewed down the *b** axis at 100 K. The patterns were generated using multiple lattice finding tool and Ewald Explorer module with twin lattices superimposed in CrysAlisPro. (c) Overlap of the two component reciprocal lattices.

The atomic positions, charge densities, and mean thermal vibrations derived from diffraction experiments are invaluable in the analysis of relative stabilities of different crystalline forms under different conditions. Atomic positions are used for lattice energy calculations, which provide a measure of the enthalpy of the system, whereas atomic displacement parameters may be used to probe the dynamics of molecular crystals. The collective vibrations of molecules in the crystals carry information about crystal entropy. Rigid-body analysis, originally proposed by Cruickshank[5] and refined by Trueblood and Schomaker to give the TLS (translation, libration, screw; correlation of translation and libration) model,[6] was developed in this context. The TLS model is based on the harmonic approximation; the molecules are considered as rigid bodies translating and librating in the harmonic mean field of the surrounding molecules in the crystal,[7] and the Debye−Waller factors are analyzed to derive the mean translational and librational motions of the molecules in the crystal. The entropy values can be derived from the low-frequency molecular vibrations based on TLS analysis.[8,9]

In this work, a systematic investigation of the temperature-induced phase transition of the title compound Boc-γ^4(*R*)Val-Val-OH was carried out. Single-crystal X-ray diffraction data sets at room temperature and 100 K were analyzed. Differential scanning calorimetry (DSC) measurements and hot-stage polarizing microscope images support the phase transition. A variable-temperature unit cell check was also carried out. A plausible mechanism for the reversible rearrangement in the crystal resulting in the phase transition is presented.

EXPERIMENTAL SECTION

Single-Crystal X-ray Diffraction. Good-quality single crystals of Boc-γ^4(*R*)Val-Val-OH were grown from a methanol/water mixture. A 0.1 mm × 0.2 mm × 0.3 mm crystal was chosen using a polarizing microscope and affixed to a Hampton Research cryoloop using Paratone N oil. Two X-ray diffraction data sets at 0.77 Å^{-1} resolution were collected on the same crystal at room temperature and 100 K on an Oxford Xcalibur (Mova) diffractometer equipped with an EOS CCD detector using Mo Kα radiation (λ = 0.71073 Å). The crystal-to-detector distance was fixed at 45 mm, and the scan width ($\Delta\omega$) was 1° per frame during the data collection. The crystal was cooled to 100 K with a liquid nitrogen stream using an Oxford Instruments Cryojet-HT nitrogen gas stream cooling device. The crystal temperature was stable to within 2 K. Cell refinement, data integration, and reduction were carried out using the program CrysAlisPro.[10] The crystal structures were solved by direct methods using SHELXS97 and refined according to the spherical-atom approximation (based on F^2) using SHELXL97[11] included in the WinGX suite.[12] Figure 1 shows the 50% probability ellipsoid plot (ORTEP[12]) of the structure of Boc-γ^4(*R*)Val-Val-OH.

At room temperature, the percentage of indexing was quite good (~90%), and the structure was solved in the orthorhombic space group $P22_12_1$ with one molecule in the asymmetric unit. However, at 100 K the percentage of indexing dropped to ~48% with a single unit cell in the monoclinic system. With the multiple unit cell finding tool in CrysAlisPro, two identical unit cells related by a 180° rotation around *a** were found, and ~80% of the total number of reflections were fitted. Multiple unit cells were visualized using the Ewald Explorer module (Figure 2). Finally, the 100 K structure was interpreted as a nonmerohedral twin generated by 180° rotation about the *a** axis, and this twin model was refined using the HKLF5 method[11] in the $P2_1$ space group with two molecules in the asymmetric unit.[13] The refinement suggested the twin components to be at the ~50% occupancy level. All of the H atoms for both the room-temperature and 100 K

dx.doi.org/10.1021/jp506874q | J. Phys. Chem. A 2014, 118, 9568−9574

structures were fixed according to the riding model (HFIX command) in WinGX. We chose an unconventional setting of $P2_12_12$ to make the unit cell axes match those of the monoclinic space group $P2_1$, thus allowing a detailed comparison of the two structures.

The reversibility of the phase transition was established by determining the unit cell parameters at different temperatures during heating and cooling cycles from 300 to 100 K in steps of 20 K on the same crystal; the step size was reduced to 5 K in the 180−230 K temperature interval in both the heating and cooling cycles.

DSC Measurements. Differential scanning calorimetry (Mettler-Toledo) was carried out using a dipeptide single crystal (1.1 mg) over the temperature range 298−133 K. The cooling and heating cycles established the reversibility of the phase transition at ∼205 K (Figure 3). The exothermic peak at

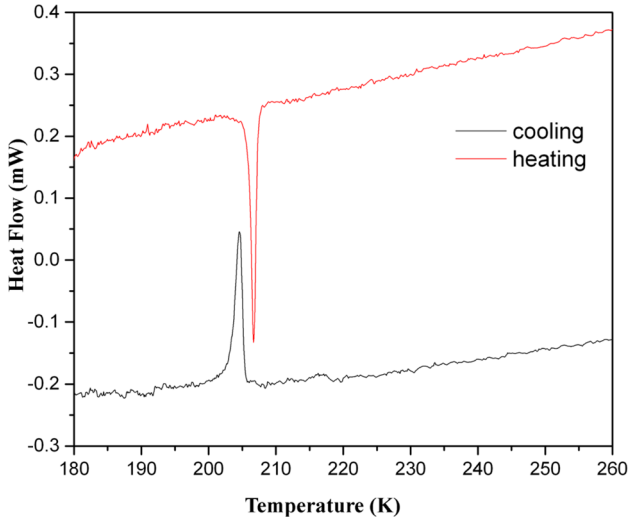

Figure 3. DSC thermograms of Boc-γ^4(*R*)Val-Val-OH for heating and cooling cycles.

205 K corresponds to an enthalpy change of 2 kJ mol^{-1}. The endothermic peak at 207 K yields an enthalpy change of 1.9 kJ mol^{-1}. The entropy associated with the transition is 10 J K^{-1} mol^{-1}. The reversibility of the transition with a 2.1 K hysteresis between the observed transition temperatures in the heating and cooling cycles is supportive of a first-order phase transition.

Hot-Stage Microscopy. A hot-stage polarizing microscope (Olympus BX-51) was used to study the thermal behavior of a single crystal of Boc-γ^4(*R*)Val-Val-OH. The same single crystal used for variable-temperature unit cell determination was placed on a slide, protected by a cover glass, during two consecutive cycles of heating and cooling from 303 to 193 K. A distinct and reversible change in the pattern of birefringence was observed at the phase transition temperature (Figure 4).

COMPUTATIONAL METHODS

Lattice energies of the orthorhombic and monoclinic forms of the peptide were calculated at the B3LYP/TZVP level[14−16] with the Grimme dispersion correction[17,18] as implemented in the CRYSTAL09 package,[19] which includes 3D periodicity. The shrinking factors (IS1, IS2, and IS3) along with the reciprocal lattice vectors were set to 4 (30 *k*-points in the irreducible Brillouin zone). The bielectronic Coulomb and exchange series values for the truncation parameter were set as ITOL1−ITOL4 = 7 and ITOL5 = 18, respectively. The level shifter was set to 0.5 hartree/cycle for better convergence.

TLS Analysis. TLS analysis was performed for all of the molecules in the asymmetric unit in both forms using the THMA11 module[20] as implemented in the WinGX package.[12] Along with the translational and librational modes of the whole molecule, internal low-frequency torsion modes of the *tert*-butyl group and isopropyl groups were analyzed. Only non-H atoms were included in this analysis because the hydrogen positions are uncertain when using X-ray diffraction data. The results of the rigid-body motion analyses[21] are given in Table S1 in the Supporting Information.

RESULTS AND DISCUSSION

Comparison of Room-Temperature and Low-Temperature Crystal Structures and Crystal Packing. The room-temperature crystal of Boc-γ^4(*R*)Val-Val-OH is orthorhombic (space group $P22_12_1$) with $Z = 4$ ($Z' = 1$). At 100 K, a monoclinic form (space group $P2_1$) with $Z = 4$ ($Z' = 2$) was obtained. The molecule in the asymmetric unit at room temperature is denoted as MOLRT (red), and the two molecules in the asymmetric unit at low-temperature are denoted as MOL1 (blue) and MOL2 (green). The unconventional setting of the space group (standard $P2_12_12$, No. 18) was chosen for the room-temperature structure to make the unit cell axes match those of the monoclinic space group $P2_1$, thus

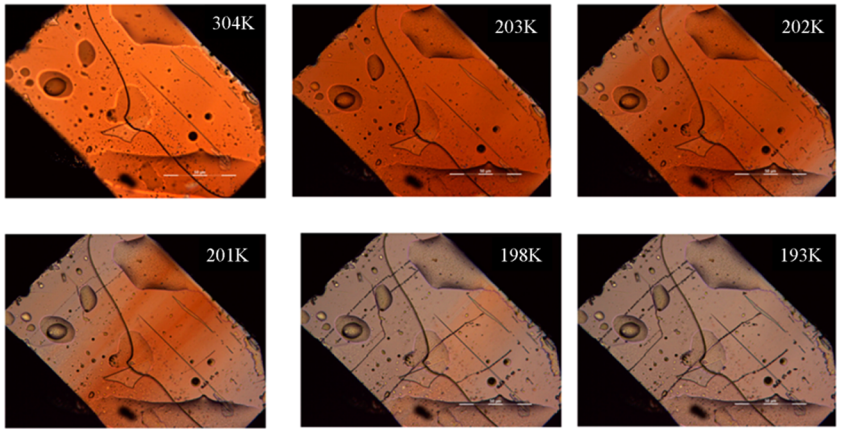

Figure 4. Hot-stage polarizing microscope images of the crystal used in data collection, supporting the observed phase change at 205 K.

dx.doi.org/10.1021/jp506874q | J. Phys. Chem. A 2014, 118, 9568−9574

Table 1. Crystallographic Parameters of Boc-γ^4(*R*)Val-Val-OH at 298 and 100 K

CCDC number	1007206	1007207
empirical formula	$C_{17}H_{32}N_2O_5$	$C_{17}H_{32}N_2O_5$
crystal habit	block shape	block shape
crystal size (mm)	0.456 × 0.303 × 0.235	0.456 × 0.303 × 0.235
crystallizing solvent	methanol	methanol
space group	$P2\ 2_1\ 2_1$	$P2_1$
a (Å)	10.1695(5)	9.868(1)
b (Å)	17.5711(6)	17.500(2)
c (Å)	12.1157(7)	12.292(1)
β (deg)	90	102.71(1)
V (Å^3)	2165.0(2)	2070.7(4)
Z	4	4
Z′	1	2
formula weight	344.45	344.45
D_{calcd} (g/cm^3)	1.057	1.105
F(000)	752	752
radiation	Mo Kα (0.71073 Å)	Mo Kα (0.71073 Å)
T (K)	298 (2)	100 (2)
θ range (deg)	2.6−26.0	2.4−26.0
measured reflns	16781	12322
observed reflns	3296	10633
$R_{obs}/wR_{2,obs}$	0.053/0.131	0.039/0.087
GoF	1.052	1.032
max/min $\Delta\rho$ (e Å^{-3})	0.129/−0.126	0.193/−0.172
data/parameter ratio	4261/225 (18.94:1)	12322/468 (26.33:1)

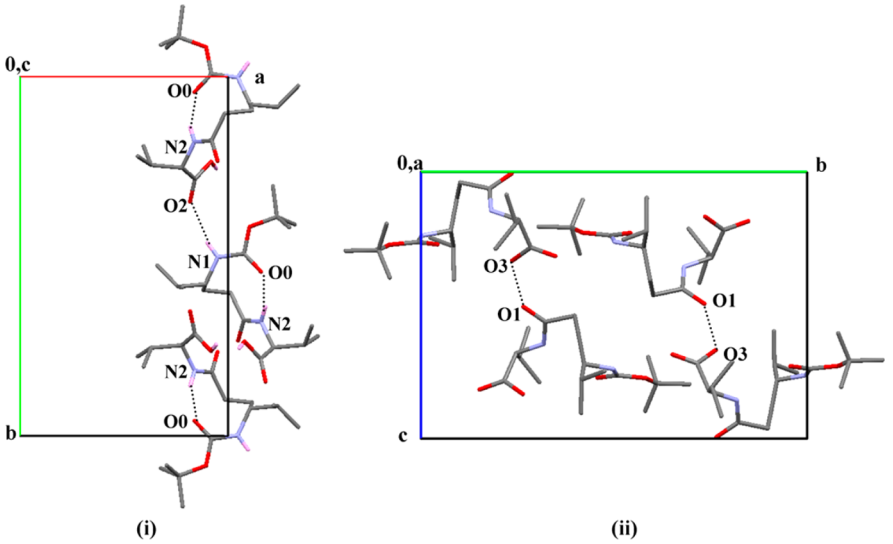

Figure 5. Packing motifs in the room-temperature form (MOLRT): (i) intra- and intermolecular N−H···O bonds along the 2_1 screw in the *b* direction; (ii) O−H···O bonds along the *c* direction.

allowing a detailed comparison of the two structures. A comparison of the crystallographic parameters of the two forms is given in Table 1.

Figure 5 shows the packing arrangement in the room-temperature orthorhombic ($P22_12_1$) form. Two types of hydrogen-bonded chains are seen. Intra- and intermolecular N−H···O hydrogen bonds link the molecules along the 2_1 screw axis parallel to the *b* axis, while O−H···O hydrogen bonds hold the network together along the 2_1 screw axis parallel to the *c* axis. The intramolecular N−H···O hydrogen bond forms a nine-atom pseudocycle (C_9) involving the γ^4(*R*)Val residue [N2···O0 in Figure 5(i)].[4] It is to be noted that only weak non-covalent interactions dominate the packing along the *a* axis and that these interactions are affected by changes in temperature.

The low-temperature monoclinic form retains the 2_1 screw along the *b* direction, whereas the 2_1 screw along the *c* direction is absent (Figure S1 in the Supporting Information). Symmetry-related molecules form separate chains of N−H···O bonds along the 2_1 screw in the *b* direction. Along the *c* axis, molecules are still linked together via O−H···O hydrogen bonds, but the molecules are no longer related by twofold rotation symmetry. Figure 6 shows an overlay diagram of the molecules in the two crystal forms (MOLRT, MOL1, and MOL2), which indicates that they nearly retain the overall molecular conformation at both temperatures. Indeed, the root-

dx.doi.org/10.1021/jp506874q | J. Phys. Chem. A 2014, 118, 9568−9574

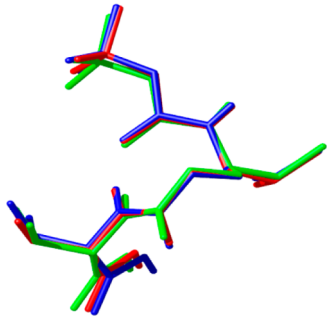

Figure 6. Diagram depicting the superposition of the three molecules MOLRT (red), MOL1 (blue), and MOL2 (green) (RMSD = 0.073).

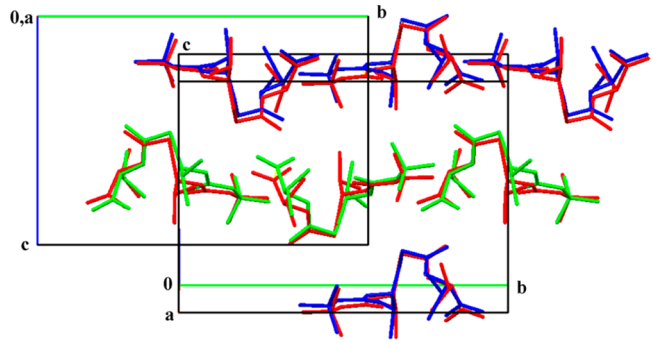

Figure 7. Packing diagrams of both forms (MOLRT in red, MOL1 in blue, and MOL2 in green) as viewed down the *a* axis, indicating the subtle changes especially at the methyl groups. These changes facilitate the observed phase transition.

mean-square deviation (RMSD) for superposition of three molecules MOLRT, MOL1, and MOL2 is 0.073 Å. It is obvious that the differences would appear only in the intermolecular packing features involving hydrogen bonds and van der Waals interactions. The N···O distances are shorter in the low-temperature monoclinic form [3.055(3) and 3.029(3) Å] since the strength of the hydrogen bond increases, whereas the O···O distances became a little *longer* [2.556(3) and 2.566(4) Å], signifying the removal of an additional symmetry restraint (Table S2 in the Supporting Information). The backbone torsion angles in MOL1 in the low-temperature monoclinic form are very close to those observed in the room-temperature orthorhombic form (MOLRT). The largest differences are observed for the Val ϕ and ψ values, with the two molecules in the monoclinic asymmetric unit deviating in opposite directions from the values observed for the room-temperature orthorhombic form by approximately $\Delta\phi \approx 17-14°$ and $\Delta\psi \approx 6°$. The largest deviation observed for the side-chain torsion angle is for Val ($\Delta\chi \approx 10°$; Table S3a–c in the Supporting Information).

A significantly large number of non-covalent interactions involving $CH_3/CH_2/CH$ groups are present in the low-temperature monoclinic form, using an interatomic distance criterion of less than or equal to the sum of the van der Waals radii + 0.2 Å (15 compared to four contacts in the room-temperature orthorhombic form). However, we performed a detailed thermal motion analysis in order to obtain greater insights into the reversible phase changes observed in the crystal. Although the hydrogen atom positions from X-ray diffraction studies are less reliable than those of C, N, and O atoms, some general features noticed in these two forms merit mention. In the case of two $CH_3\cdots CH_3$ contacts [one involving the $\gamma^4(R)$Val residues and the other involving Val and Boc units; Table S4 in the Supporting Information], the H···H distances increase while the C···C distances decrease upon cooling (Figure S2 in the Supporting Information). The CH_3 groups cluster along the *ac* plane of the unit cell, and relatively small displacements of the molecules in the unit cell with the variation of temperature (Figure 7) are sufficient to induce the reversible phase transition without disruption of the single-crystalline nature. Notably, the *a* and *c* axis lengths show small but significant changes with varying temperature, whereas the *b* axis length remains almost unchanged. These observations[4] tend to support the observed reversible phase transition.

Thermal Evolution of the Lattice Parameters. A variable-temperature unit cell determination over the temperature range of 300–100 K at intervals of 20 K, with the interval reduced to 5 K near the transition temperature, depicts the evolution of the cell parameters as shown in Figure 8. From 300 to 220 K, the crystal system is orthorhombic. Below 205 K, the

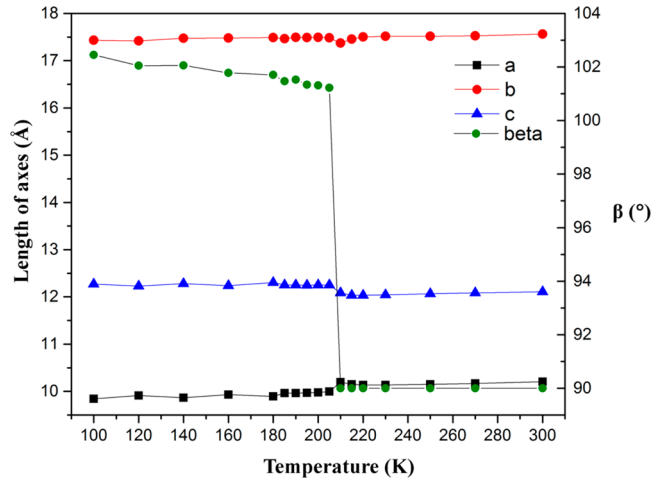

Figure 8. Temperature dependence of the unit cell parameters (*a*, *b*, and *c* axes and the angle β). Changes are seen at the transition temperature.

crystal system undergoes a transition to a nonmerohedral twin monoclinic system. The cell parameters display an abrupt jump near the transition temperature (205–210 K), consistent with the DSC measurements. During the cooling cycle, the angle β shows the largest variation from 90° to 101.2° ($\Delta\beta/\beta$ = 12.47%), while the *a* cell axis decreases by 1.95% ($\Delta a/a$), the *c* axis increases by 1.40% ($\Delta c/c$), and the *b* axis remains almost constant ($\Delta b/b$ = 0.65%). The overall decrease in volume is $\Delta V/V$ = 1.82%. This behavior clearly indicates that small changes in the relative positions of the molecules are mostly concentrated in the *ac* plane. Subtle differences between the heating and cooling cycles occur, although the trend remains the same.

Contributions from Translational and Librational Modes to the Solid-State Entropies. The reversibility of the phase transition led us to explore possible differences in the thermal motion of Boc-$\gamma^4(R)$Val-Val-OH and compare the solid-state entropies of the two crystal forms. There is a systematic difference in the magnitudes of the atomic displacement parameters of non-H atoms as a function of temperature (Figure 9). As expected, the differences are pronounced for the CH_3 groups of the Boc and Val residues.

dx.doi.org/10.1021/jp506874q | J. Phys. Chem. A 2014, 118, 9568–9574

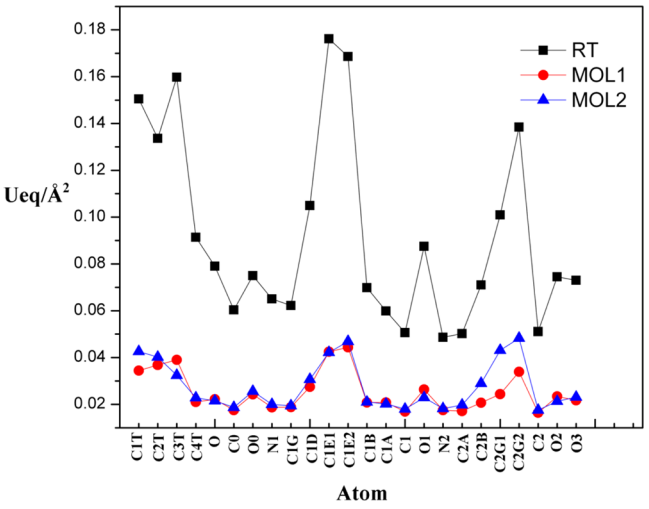

Figure 9. Equivalent isotropic displacement parameters U_{eq} for non hydrogen atoms, indicating the trends in both crystal forms.

It is to be noted that while the entire molecule was treated as a rigid group, the Boc and isopropyl groups of the Val and $\gamma^4(R)$Val residues were treated as nonrigid groups in the TLS analysis using THMA11.[20] An examination of Table 2, which

Table 2. Frequencies of the Three Translational, Three Librational, and Three Torsional Modes Obtained from TLS Analysis

	ν (cm^{-1})		
mode	MOLRT	MOL1	MOL2
T1	16.9	19.6	17.6
T2	19.2	20.4	19.7
T3	23.0	22.7	20.5
L1	24.2	26.2	26.2
L2	33.5	33.3	45.8
L3	78.2	124.2	0.0[a]
γVal	69.6	98.6	53.5
Val	50.6	76.5	65.5
Boc	48.8	60.0	56.6

[a]The negative value was reset to 0.0.

lists the translational, librational, and torsional frequencies associated with the two crystal forms, suggests that in general the frequency of the L3 mode shows significant changes in the two molecules of the monoclinic form compared with the orthorhombic form (Figure S3 in the Supporting Information). Furthermore, it is to be noted that the L3 mode of MOL2 gets reset to 0.0 cm^{-1} as the corresponding eigenvalue becomes negative. The torsional mode frequencies for the Boc and Val residues increase in the monoclinic form compared with the orthorhombic form, while the torsional frequency for the $\gamma^4(R)$Val residue increases for MOL1 but decreases for MOL2 (Table 2).

The crystal-state entropies were estimated using the approach described by Madsen and Larsen[8] (Table 3 and Figure 10). The calculations were performed by assuming that the molecules in the monoclinic form were also at 298 K, which fits in within the harmonic approximation. This resulted in estimated entropy values of S_{MOLRT}(298 K) = 207.7 J mol^{-1} K^{-1}, S_{MOL1}(298 K) = 193.7 J mol^{-1} K^{-1}, and S_{MOL2}(298 K) = 187.2 J mol^{-1} K^{-1}.

Table 3. Solid-State Entropies at 298 K

	S (J mol^{-1} K^{-1})		
mode	MOLRT	MOL1	MOL2
T1	29.1	27.9	28.8
T2	28.1	27.6	27.9
T3	26.6	26.7	27.5
L1	26.2	25.5	25.5
L2	23.5	23.5	20.9
L3	16.5	12.7	0.0
Boc	20.3	18.6	19.1
γVal	17.4	14.6	19.6
Val	20.0	16.6	17.9
total	207.7	193.7	187.2

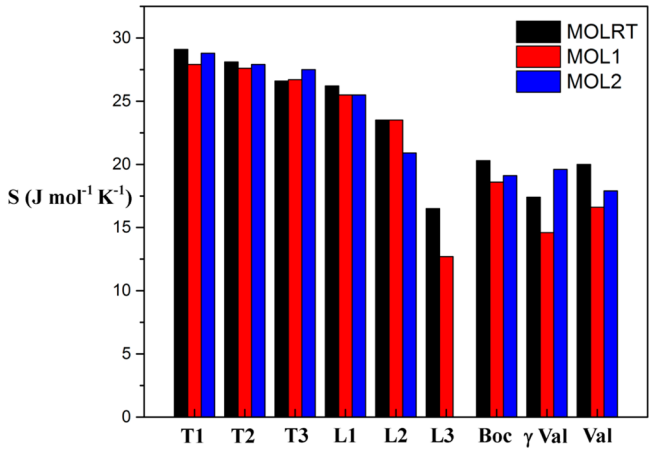

Figure 10. Histogram showing the solid-state entropies related to the three translational, three librational, and three torsional modes in the crystals.

Interplay of Enthalpy and Entropy in the Reversible Phase Transition. The reversibility of the phase transition suggests that enthalpy−entropy compensation is involved in determining the free energies of the two crystal forms. Lattice energy calculations were carried out using the periodic code in CRYSTAL09 (Table 4). The comparison at the molecular level

Table 4. Lattice Energies (E) Calculated Using the CRYSTAL09 Package

	E (kJ mol^{-1})	ΔE (kJ mol^{-1})[a]
MOLRT	−185.56	0.0
MOL1	−193.10	−7.54
MOL2	−188.93	−3.37

[a]$\Delta E = E - E_{MOLRT}$.

indicates that MOL1 is stabilized by 7.5 kJ mol^{-1} and MOL2 is stabilized by 3.4 kJ mol^{-1} relative to MOLRT. Thus, while it is clear that the enthalpic contributions favor a stable monoclinic form, the entropic features indicate the contrary. Hence, the subtle interplay of these two factors ensures the reversibility of the two crystal forms with temperature.

CONCLUSION

The temperature induced reversible first-order phase transition in the dipeptide Boc-$\gamma^4(R)$Val-Val-OH is characterized as being driven by an interplay of enthalpy and entropy across the phase transition temperature. This analysis in peptides that are held

dx.doi.org/10.1021/jp506874q | J. Phys. Chem. A 2014, 118, 9568−9574

together by strong hydrogen-bonded motifs, including the intramolecular "C_9-type" N−H···O interactions, brings out the importance of temperature-induced behavior in such systems. The results suggest that subtle balancing of thermodynamic parameters may be critical in determining organic crystal structures stabilized predominantly by weak interactions and that reversible phase transitions may not be entirely uncommon. Furthermore, this study offers a possible probe for the analysis of subtle phase changes observed in biological systems.

■ ASSOCIATED CONTENT

Supporting Information

Crystallographic information files (CIF); Figures S1−S3 showing packing diagrams and normal modes from TLS analysis; and Tables S1−S4 containing thermal motion analysis results from the THMA11 program, hydrogen-bond geometries and non-covalent intermolecular interactions, and backbone torsion angles of the molecules in the asymmetric unit in the two crystal forms. This material is available free of charge via the Internet at http://pubs.acs.org.

■ AUTHOR INFORMATION

Notes

The authors declare no competing financial interest.

■ ACKNOWLEDGMENTS

R.P. was supported by a Senior Research Fellowship from the Council of Scientific and Industrial Research, India. T.N.G.R. thanks the Department of Science and Technology for the award of a J. C. Bose Fellowship.

■ ABBREVIATIONS

Boc, *tert*-butyloxycarbonyl; $\gamma^4(R)$Val, (*R*)-4-amino-5-methylhexanoic acid; Boc-$\gamma^4(R)$Val-Val-OH, ((*R*)-((*tert*-butoxycarbonyl)amino)-5-methylhexanoyl)-L-valine

■ REFERENCES

(1) Barbour, L. J. Single crystal to single crystal transformations. *Aust. J. Chem.* **2006**, *59*, 595−596.
(2) Moggach, S. A.; Parsons, S.; Wood, P. A. High-pressure polymorphism in amino acids. *Crystallogr. Rev.* **2008**, *14*, 143−184.
(3) Moggach, S. A.; Lennie, A. R.; Morrison, C. A.; Richardson, P.; Stefanowicz, F. A.; Warren, J. E. Pressure induced phase transitions in the tripeptide glutathione to 5.24 GPa: The crystal structure of glutathione-II at 2.94 GPa and glutathione-III at 3.70 GPa. *CrystEngComm* **2010**, *12*, 2587−2595.
(4) Vasudev, P. G.; Chatterjee, S.; Shamala, N.; Balaram, P. Structural Chemistry of Peptides Containing Backbone Expanded Amino Acid Residues: Conformational Features of β, γ, and Hybrid Peptides. *Chem. Rev.* **2011**, *111*, 657−687.
(5) Cruickshank, D. The analysis of the anisotropic thermal motion of molecules in crystals. *Acta Crystallogr.* **1956**, *9*, 754−756.
(6) Schomaker, V.; Trueblood, K. N. On the rigid-body motion of molecules in crystals. *Acta Crystallogr., Sect. B* **1968**, *24*, 63−76.
(7) Trueblood, K. N.; Dunitz, J. D. Internal molecular motions in crystals. The estimation of force constants, frequencies and barriers from diffraction data. A feasibility study. *Acta Crystallogr., Sect. B* **1983**, *39*, 120−133.
(8) Madsen, A. Ø.; Larsen, S. Insight into Solid-State Entropy from Diffraction Data. *Angew. Chem., Int. Ed.* **2007**, *46*, 8609−8613.
(9) Madsen, A. Ø.; Mattson, R.; Larsen, S. Understanding Thermodynamic Properties at the Molecular Level: Multiple Temperature Charge Density Study of Ribitol and Xylitol. *J. Phys. Chem. A* **2011**, *115*, 7794−7804.
(10) *CrysAlisPro CCD, CrysAlisPro RED, ABSPACK, and CrysAlis PRO*; Agilent Technologies: Yarnton, England, 2010.
(11) Sheldrick, G. A short history of SHELX. *Acta Crystallogr., Sect. A* **2008**, *64*, 112−122.
(12) Farrugia, L. J. WinGX and ORTEP for Windows: An update. *J. Appl. Crystallogr.* **2012**, *45*, 849−854.
(13) Herbst-Irmer, R.; Sheldrick, G. M. Refinement of Twinned Structures with SHELXL97. *Acta Crystallogr., Sect. B* **1998**, *54*, 443−449.
(14) Becke, A. D. Density-functional thermochemistry. III. The role of exact exchange. *J. Chem. Phys.* **1993**, *98*, 5648−5652.
(15) Lee, C.; Yang, W.; Parr, R. G. Development of the Colle−Salvetti correlation-energy formula into a functional of the electron density. *Phys. Rev. B* **1988**, *37*, 785−789.
(16) Peintinger, M. F.; Oliveira, D. V.; Bredow, T. Consistent Gaussian basis sets of triple-zeta valence with polarization quality for solid-state calculations. *J. Comput. Chem.* **2013**, *34*, 451−459.
(17) Grimme, S. Semiempirical GGA-type density functional constructed with a long-range dispersion correction. *J. Comput. Chem.* **2006**, *27*, 1787−1799.
(18) Brandenburg, J. G.; Alessio, M.; Civalleri, B.; Peintinger, M. F.; Bredow, T.; Grimme, S. Geometrical correction for the inter- and intramolecular basis set superposition error in periodic density functional theory calculations. *J. Phys. Chem. A* **2013**, *117*, 9282−9292.
(19) Dovesi, R.; Saunders, V.; Roetti, C.; Orlando, R.; Zicovich-Wilson, C.; Pascale, F.; Civalleri, B.; Doll, K.; Harrison, N.; Bush, I. *CRYSTAL09 User's Manual*; University of Torino: Torino, Italy, 2009.
(20) Maverick, T.; Trueblood, K. *Thermal Motion Analysis Program THMA-11*; Zurich, Switzerland, 1987.
(21) Seiler, P.; Dunitz, J. D. Redetermination of the ruthenocene structure at room temperature and at 101 K: Molecular internal motion. *Acta Crystallogr., Sect. B* **1980**, *36*, 2946−2950.